ISSN: 2688-8645

Modeling and Docking Trajectory Optimization of LNG Loading Arm Based on Modified D-H Method

Quancheng Dong [1], Faguang Jiang [2], Kebing Cheng [2]

[1] School of Mechanical Engineering, Southwest Petroleum University, Chengdu Sichuan, 610500, China

[2] School of Mechanical Engineering, Southwest Petroleum University, Guangzhou Guangdong, 615000, China

Abstract

Aiming at the low accuracy and poor stability of manual docking for 5-axis LNG loading arms, this paper focuses on its kinematic modeling and docking trajectory planning optimization. First, the hydraulic-driven LNG loading arm was simplified into a 5-joint robotic arm model with a virtual joint, and its kinematic model was established based on the Modified Denavit-Hartenberg (M-DH) method. A D-H parameter table was constructed, and the safe rotation range of each joint was defined via motion interference analysis. Considering the large mass-span ratio of the LNG loading arm, joint space trajectory planning was adopted. Four interpolation algorithms (cubic/quintic spline, cubic/quintic polynomial) were compared and simulated by Matlab Robotics Toolbox, with the motion characteristics of the end effector and joints evaluated. The results show that the quintic polynomial interpolation algorithm is optimal: it generates a continuously differentiable spatial arc trajectory in Cartesian space with C^4 continuity of position, velocity and acceleration in the time domain. The joint motion is smooth without abrupt changes, the jerk index meets engineering requirements, and the trajectory has high fault tolerance. This study provides a reliable kinematic model and optimal trajectory scheme for the automatic docking of LNG loading arms, offering theoretical and technical support for its automation transformation and high-precision controller design.

Keywords

LNG Loading Arm; Modified D-H Method; Kinematic Modeling; Trajectory Planning; Quintic Polynomial Interpolation; Joint Space.

1. Introduction

At present, road transportation is a typical land transportation mode in the LNG logistics system. When filling LNG tank trucks, the manual docking of the filling arm pipe and the tank opening is generally adopted, which restricts the efficiency of LNG filling into tank trucks, and has the disadvantages of low docking accuracy, high operation intensity and poor safety. Therefore, it is urgent to improve the automation level of LNG filling. In the process of automatic filling of the LNG filling arm, the trajectory planning and trajectory tracking of automatic docking play a decisive role.

Scholars have conducted extensive research on trajectory planning. Ye Dai[1] t al. introduced the research status of motion trajectory planning and discussed the basic principles and practical applications of trajectory planning methods for space robotic arms. Yang,Mei[2] et al. analyzed the structural characteristics of the internal space of the shield machine and determined the installation position of the robot and the distribution area of the cutters to be replaced. Zhao yanling[3] et al. built a ROS simulation platform to simulate the joint motion

ISSN: 2688-8645

planning of the winding robot and verify the principle and feasibility of the multi-wire parallel winding hybrid robot. Li Hao[4] et al. solved the difficulties in the implementation of industrial robot trajectory planning algorithms and realized the ideal motion trajectories of six-axis industrial robots in Cartesian space and joint space based on the ROS platform.

At present, polynomial interpolation trajectory planning is the mainstream for the trajectory planning of multi-axis robotic arms in space. Ren Jun [5] et al. took the ER50 robot as the main research equipment, adopted the quintic polynomial interpolation algorithm to carry out the simulation of point-to-point trajectory planning in space for the ER50 robot, and successfully generated a smooth trajectory curve. Cai Guoqing[6] et al. used the quintic polynomial interpolation method to plan the end trajectory of the robot to improve the tracking control ability of the food handling robot for trajectory interpolation points during continuous and stable motion, and verified the effectiveness of the method through experiments. Gao Zhengrui[7] et al. studied the trajectory optimization problem of the ER10-1600 six-axis robot to ensure the stable and safe operation of the robot and its adaptation to complex working environments, and adopted cubic and quintic polynomial planning methods to solve the stability problem and optimize it.

Aiming at the problems of low manual docking accuracy and difficulty in ensuring high-quality task completion for existing LNG loading arms, this paper explores the optimal docking trajectory from the LNG loading arm to the tank truck flange from multiple perspectives, providing an important solution for the automatic filling system of LNG loading arms.

2. Establishment of Kinematic Model for LNG Loading Arm

2.1. Simplification of LNG Loading Arm Model

This paper takes a 5-axis LNG loading arm as the research object, and the on-site equipment is shown in Figure 1. At present, the loading arm is manually guided to dock with the LNG tank truck, which cannot guarantee the loading efficiency, docking accuracy and the safety of operators. Therefore, the transformation and upgrading of the LNG loading arm into automatic equipment is an urgent need in engineering practice and conforms to the trend of industrial development.

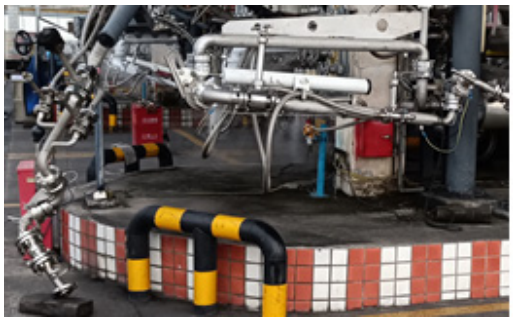

Figure 1. On-site view of LNG loading arm

At present, the driving methods of industrial robotic arms mainly include hydraulic drive, pneumatic drive, electric drive, magnetostrictive drive and shape memory alloy drive[8].

Due to the self-weight of the LNG loading arm, hydraulic drive and electric drive are the two preferred driving methods, both of which can provide large driving torque. Considering the cost and the environment of the LNG receiving station, hydraulic drive is selected. The upgraded LNG loading arm is shown inFigure 2 which consists of a column, an inner arm, an outer arm, a driving part, a stop valve and a connecting unit. The movement of the LNG loading arm is realized by 5 rotating joints, among which 3 move perpendicular to the ground and 2 move parallel to the ground.

ISSN: 2688-8645

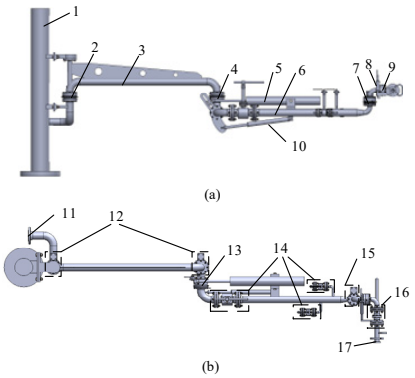

1. Column 2. Inner arm drive 3. Inner arm 4. Outer arm vertical drive 5. Spring cylinder balancing device 6. Outer arm 7. Connecting pipe vertical drive 8. Connecting pipe hydraulic rod 9. Connecting pipe horizontal drive 10. Outer arm hydraulic rod 11. Liquid phase interface 12. Inner arm hydraulic motor 13. Outer arm horizontal drive 14. Stop valve 15. Connecting unit hydraulic motor 16. Breakaway valve 17. Docking flange

Figure 2. LNG loading arm (a) Front view (b)Top view

To simplify the model to the greatest extent, only the main components of the LNG loading arm for completing the docking task are retained, and the LNG loading arm is abstracted as a 5-axis robotic arm, and the research model of this paper is obtained as shown in Figure 3.

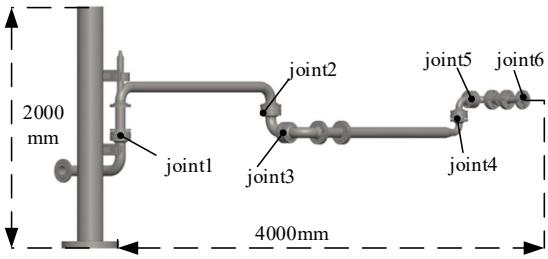

Figure 3. Simplified model of LNG loading arm

The LNG loading arm is an integral chain structure, and the overall movement is controlled by 5 rotating joints without translational joints. The simplified model of the LNG loading arm sets 6 joints (joint1~joint6), among which joint1~joint5 are the rotating joints of the LNG loading arm. To facilitate the acquisition of the end position and posture of the LNG loading arm, a virtual joint joint6 is added, which is set as the docking flange at the end of the loading arm.

2.2. Kinematic Modeling of LNG Loading Arm

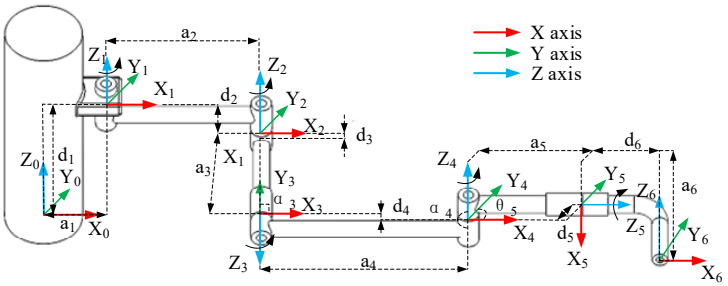

Figure 4. D-H parameter model of LNG loading arm

The modified Denavit-Hartenberg (M-DH) method includes four parameters, two of which are used to describe the connecting rod, and the other two are used to describe the relative position

ISSN: 2688-8645

relationship between two adjacent connecting rods. Therefore, based on the M-DH method, a reference coordinate system {A0} is established with the model column as the reference, and the kinematic model of the loading arm as shown in Figure 4 is built.

Table 1. D-H parameter table of LNG loading arm

Link i	θ_i(°)	d_i(mm)	a_{i-1}(mm)	α_{i-1}(°)	Variable range
1	θ_1	957	360	0°	90°~90°
2	θ_2	210	1790	0°	60°~90°
3	θ_3	-242	242	90°	20°~90°
4	θ_4	180	1854	90°	90°~90°
5	θ_5	94	179	90°	180°~180°
6	θ_6	530	94	90°	180°~180°

Except for the column reference coordinate system, the origin of the coordinate system of other joint is set at the centroid of each rotating joint. Combined with the analysis of the simplified model in Figure 3, joint1, joint2 and joint4 move perpendicular to the ground, so their axes are arranged vertically, and the positive direction of motion is defined as counterclockwise from the top view; joint3 and joint5 move parallel to the ground, their joint axes are arranged horizontally, and the positive direction of motion is defined as clockwise into the paper; joint6 is a virtual joint, and the coordinate system direction is set to be consistent with the reference coordinate system. The link parameters of each joint itself, including link length ai and link torsion angle αi, as well as the relative position parameters of adjacent links, including link length difference (offset distance) di and link angular displacement (joint angle) θi, and the rotation direction of each joint are marked in Figure 5, and the D-H parameter table of the LNG loading arm is obtained as shown in Table 1.

The column reference coordinate system {A0} is a fixed coordinate system, so it is not listed in Table 1. The variable range in Table 1 represents the rotation angle range of each joint. A safe rotation angle (-90°~90°) is set for joint1 considering the interference with the column, and a safe rotation angle (-60°~90°) is also set for joint2 because an excessive rotation angle will cause interference with joint1. An excessive clockwise rotation angle of joint3 will cause joint6 to collide with the ground, so a theoretical calculation model for the rotation angles of joint3~5 is established.

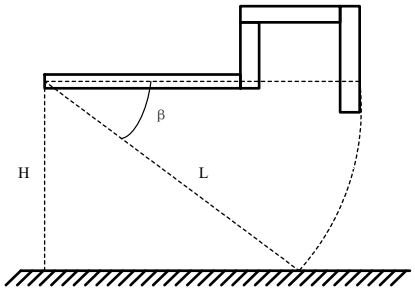

Figure 5. Calculation model of rotation angles of joint3~5

In Figure 5, H represents the height of joint3 from the ground, L represents the distance from joint3 to joint6, and β represents the limit angle of joint3 rotation. It can be obtained from Figure 5:

ISSN: 2688-8645

$$\sin\beta = \frac{H}{L} \tag{1}$$

Based on the formulas and Table 1, the following can be calculated:

$$\beta \approx 28^{\circ} \tag{2}$$

To ensure equipment safety, the maximum clockwise rotation angle of joint3 is set to 20°. Since joint3 is controlled by a hydraulic rod, the maximum counterclockwise rotation angle is set to 90°.

3. Trajectory Planning of LNG Loading Arm

The trajectory planning of robotic arms can be divided into Cartesian space path planning and joint space path planning. The mass and span ratio of the LNG loading arm are larger than those of common industrial robotic arms, so joint space trajectory planning is more in line with the working conditions of the LNG loading arm. In this section, cubic spline, quintic spline, cubic polynomial and quintic polynomial are compared and referenced to obtain the optimal trajectory.

3.1. Spline Interpolation Trajectory

3.1.1. Cubic Spline Interpolation Trajectory

According to the on-site actual measurement of the LNG loading arm, the initial position of the end effector in the Cartesian coordinate system is (4.495, -0.36, -0.105), the target position is (1.5, 1.5, 1.5), and it is stipulated to move from the initial position to the target position within 4 seconds. Cubic spline interpolation is performed on the x, y, z directions and time respectively to ensure the same dimension of position and time. The pose of the end effector in the x, y, z directions with respect to time is obtained through matrix operation, and the velocity and acceleration of the end effector moving from the initial position to the target position within 0~4s are obtained by the first and second gradient operations of the obtained pose matrix, as shown in Figure 6.

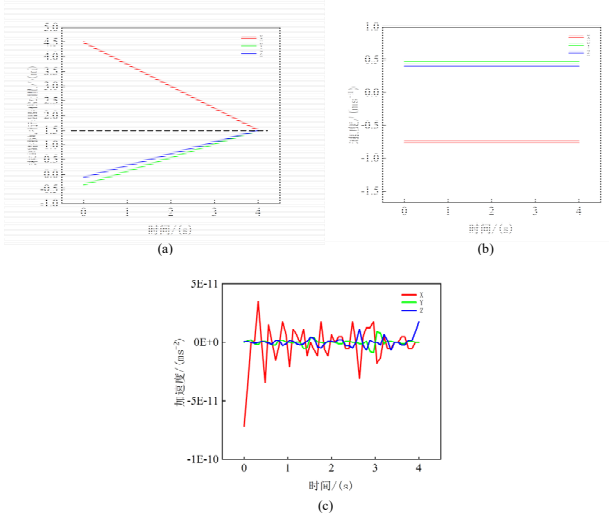

Figure 6. Cubic spline interpolation trajectory (a) End effector position (b) Velocity (c) Acceleration

It can be seen from Figure 6(a) that the end effector finally reaches the target position (1.5, 1.5, 1.5), and the movement of the end effector in the x, y, z directions shows a linear decrease. In Figure 6 (b), the end effector moves at a constant speed of -0.75m/s, 0.47m/s and 0.4m/s in the x, y, z directions respectively; in Figure 6 (c), there is a step phenomenon in the x, y, z directions of the end effector, with a large fluctuation in the x direction and small fluctuations in the y and

ISSN: 2688-8645

z directions, but the overall fluctuation can be ignored. Obviously, this is not in line with engineering practice. The LNG loading arm is initially in a static state, and in the velocity diagram of Figure 6 (b), the LNG loading arm has no acceleration and deceleration stages and moves almost at a constant speed. The joint angles of the loading arm are obtained by the inverse kinematics equation solution method, and the trajectory of the LNG loading arm planned by cubic spline interpolation is drawn as shown in Figure 7.

In the trajectory diagram of Figure 7, the trajectory of the LNG loading arm is a spatial straight line, which is consistent with the position change in Figure 6 (a). However, in engineering practice, achieving the trajectory in Figure 7 requires high motion control accuracy.

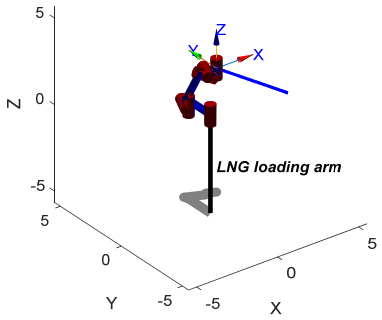

Figure 7. Cubic spline interpolation trajectory

To sum up, although the cubic spline interpolation trajectory planning can reach the target position, the velocity during the docking process is not in line with the actual situation and the subsequent control is very difficult. Therefore, the cubic spline interpolation trajectory planning does not meet the requirements.

3.1.2. Quintic Spline Interpolation Trajectory

The motion parameters of cubic spline interpolation trajectory planning during the docking process are too ideal, because the cubic spline interpolation trajectory planning method only takes the initial position, target position and time as the boundaries. Therefore, the quintic spline interpolation with a higher order is considered to plan the automatic docking trajectory of the LNG loading arm.

The main feature of quintic spline interpolation trajectory planning is that it has continuous velocity and acceleration at the initial and target positions, making it smoother and more stable in application than the simpler cubic spline interpolation[9].

The quintic spline interpolation trajectory planning also sets the initial position and target position as (4.495, -0.36, -0.105) and (1.5, 1.5, 1.5) with a planning time of 4 seconds. The position, velocity and acceleration of the end effector of the LNG loading arm moving from the initial position to the target position are shown in Figure 8.

It can be seen from Figure 8 (a) that the end effector of the LNG loading arm reaches the target position (1.5, 1.5, 1.5); compared with the velocity of the cubic spline interpolation trajectory, the velocity in Figure 8 (b) is smoother, but the velocity at the initial and final positions is still not zero; the acceleration diagram in Figure 8 (c) has a changing trend compared with the cubic spline interpolation trajectory, which is more in line with the actual situation, but the acceleration of the LNG loading arm has an abrupt change at the moment of starting to move from the initial position and approaching the target position, which indicates that there is an impact on the LNG loading arm at this time.

ISSN: 2688-8645

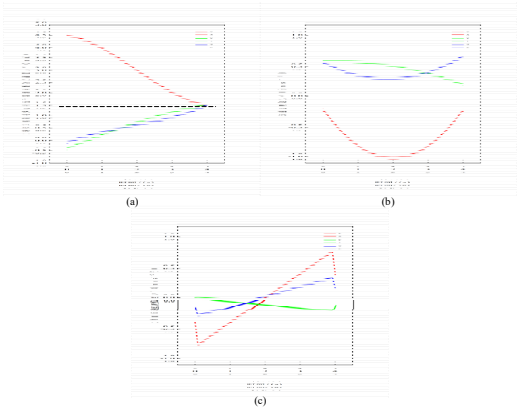

Figure 8. Quintic spline interpolation trajectory (a) End effector position (b) Velocity (c) Acceleration

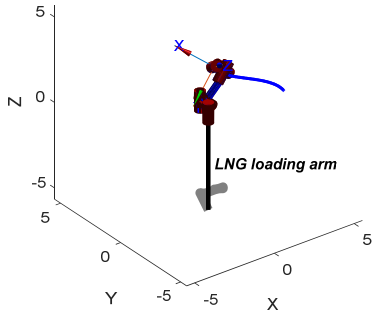

Figure 9. Quintic spline interpolation trajectory

Figure 9 shows the quintic spline interpolation trajectory, which is smoother than the cubic spline interpolation, and the climbing of the end effector in the z direction is more gentle. However, the quintic spline interpolation trajectory planning still does not meet the expected trajectory because the velocity at the initial and final positions is not zero and the acceleration has an abrupt change at the moment of starting to move and approaching the target position.

3.2. Polynomial Interpolation Trajectory

3.2.1. Cubic Polynomial Interpolation Trajectory

Both spline interpolation trajectory planning methods have the problem that the velocity at the initial and final positions is not zero, which is inconsistent with the actual situation, because spline interpolation is suitable for the planning of multi-segment trajectories. However, the trajectory of the LNG loading arm has only two points: the initial position and the target position, which is not suitable for multi-segment trajectories. Polynomial interpolation trajectory is suitable for the trajectory planning of a single interval and is simpler to implement15].Therefore, the polynomial interpolation trajectory planning for a single trajectory is considered to plan the LNG loading and docking trajectory, and the cubic polynomial interpolation trajectory is first used for planning.

The initial position and target position of the LNG loading arm trajectory are known, the initial velocity and final velocity are set to 0, and the planning time is also set to 4 seconds. The x, y, z directions are decomposed and solved simultaneously, and the position, velocity and acceleration diagrams of the end effector with cubic polynomial interpolation are obtained as shown in Figure 10.

ISSN: 2688-8645

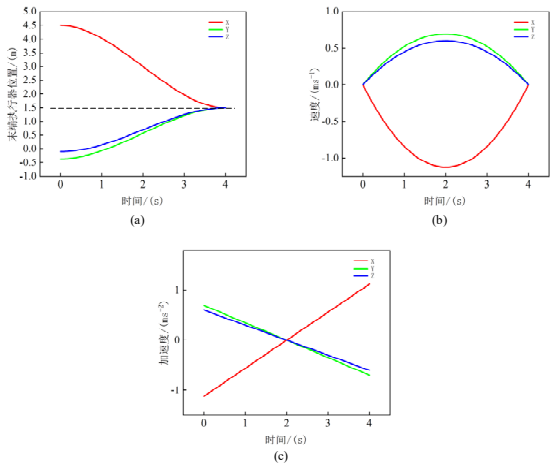

Figure 10. Cubic polynomial interpolation (a) End effector position (b) Velocity (c) Acceleration

It can be seen from the position diagram in Figure 10 (a) that the LNG loading arm reaches the specified target position (1.5, 1.5, 1.5)， Figure 10 (b) is the velocity diagram: the velocity of the LNG loading arm in the x direction increases from 0 m/s to the negative maximum and then gradually decreases to 0 m/s, reaching the negative maximum at 2 seconds; the y and z directions have the same trend and also reach the maximum velocity at 2 seconds. Figure 10 (c) is the acceleration diagram: during the docking process, the acceleration of the LNG loading arm increases linearly in the x direction and decreases linearly in the y and z directions, and the acceleration is the maximum at the initial and final positions as a whole.

Figure 11 shows the cubic polynomial trajectory, which is a spatial straight line, the same as the cubic spline interpolation, which has high requirements for the motion controller.

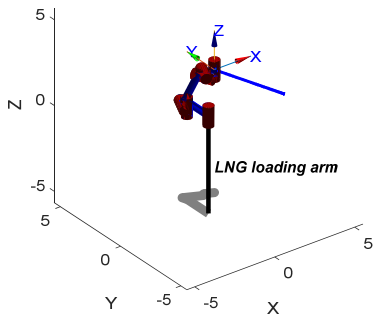

Figure 11. Cubic polynomial interpolation trajectory

To intuitively observe the trajectory of the LNG loading arm during the docking process, the position, velocity and acceleration diagrams of each joint are obtained by the inverse kinematics equation, as shown in Figure 12,Figure 13 and Figure 14.Figure 12 is the position diagram of each joint: the positions of joint1~6 are continuous during the docking process. The virtual joint joint6 does not move because the position accuracy is prioritized during the docking process at the expense of the posture control of joint6; for joint1~5, there are varying degrees of position abrupt changes and fluctuations at 3~4 seconds when approaching the target position. Among them, the oscillation of joint4 is small and can be regarded as smooth movement; while joint5 oscillates twice in the time period from 3.27s to 3.51s, with the position abruptly changing from -3.14rad to 2.88rad, which means that the position of joint5 reverses by nearly 180° within 0.14s, which seriously affects the stability of the automatic docking of the

ISSN: 2688-8645

LNG loading arm and the service life of the rotating joints. In the position diagram of each joint, the abrupt changes of joint1~4 are within the acceptable range, but the nearly 180° reversal of joint5 in a short time is unacceptable and does not meet the requirements.

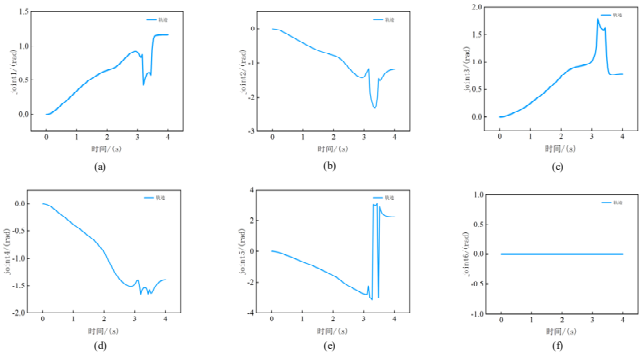

Figure 12. Joint positions

The overall trends of the joint velocity diagram in Figure 13 and the joint acceleration diagram in Figure 14 are similar. Consistent with the joint position diagram in Figure 12, the virtual joint joint6 is in a static state, and the velocity and acceleration of other joints all oscillate and have sharp points in the time period from 3s to 4s. Different from the joint position diagram in Figure 12, joint1~5 of the LNG loading arm move gently at a low speed in the time period from 0~3s, and have a large amplitude oscillation when approaching the target position, and finally the velocity tends to 0. The velocity fluctuation ranges of joint1~3 are similar, joint4 has the smallest fluctuation, while joint5 has a very large fluctuation range. Different from the joint velocity diagram in Figure 13, the overall fluctuation range of each joint in the acceleration diagram in Figure 14 is very large, and the fluctuation range of joint5 even reaches 11227.03rad/s^2. The results show that the cubic polynomial interpolation trajectory planning is not suitable for the LNG loading arm.

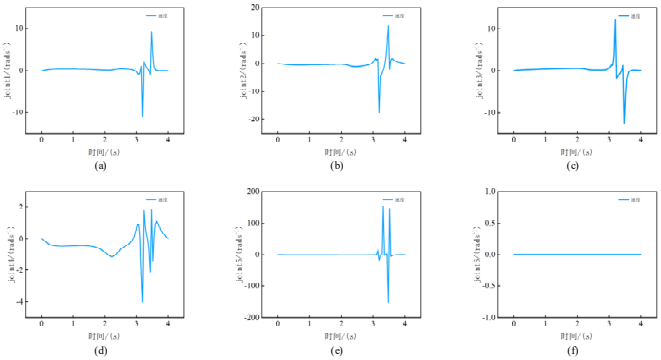

Figure 13. Joint velocities

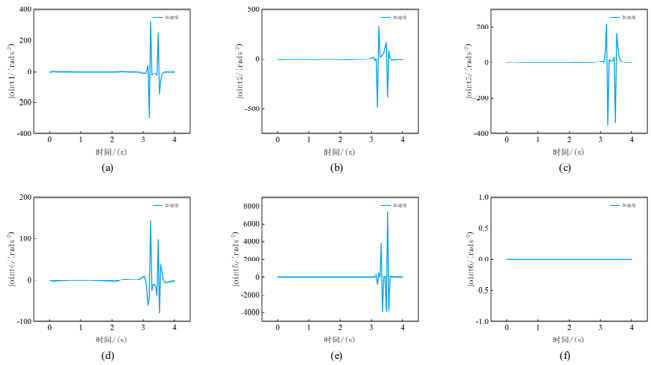

Figure 14. Joint accelerations

ISSN: 2688-8645

3.2.2. Quintic Polynomial Interpolation Trajectory

The performance of each motion parameter of the LNG loading arm during the docking process is poor in cubic polynomial interpolation trajectory planning, because the cubic polynomial interpolation does not control the acceleration, and abandons the posture control of the end effector to ensure the position accuracy. For this reason, a higher-order quintic polynomial interpolation is selected to plan the automatic docking trajectory. In addition to satisfying the position and velocity conditions, the quintic polynomial interpolation trajectory can also control the initial and final acceleration of the trajectory, making the trajectory smoother[10].

The initial position and target position of the LNG loading arm trajectory are known, the initial velocity, final velocity, initial acceleration and final acceleration are set to 0, and the planning time is set to 4 seconds. The x, y, z directions are decomposed and solved simultaneously, and the position, velocity and acceleration diagrams of the end effector with quintic polynomial interpolation are obtained as shown in Figure 15.

Figure 15 (a) is the position diagram of the end effector: the LNG loading arm finally moves to the target position (1.5, 1.5, 1.5) within the planning time. Figure 15 (b) is the velocity diagram of the end effector: the velocity at the initial and final positions is 0 m/s, the end effector shows a sinusoidal fluctuation in the Y and Z directions and reaches the maximum velocity at 1.41s and 1.54s respectively; the X direction shows a cosine fluctuation and reaches the negative maximum velocity at 2.14s. Figure 15 (c) is the acceleration diagram of the end effector: the acceleration at the initial and final positions is 0 m/s^2, the change trend of the acceleration diagram is the same as that of the velocity diagram, the Y and Z directions show sinusoidal fluctuations, and the X direction shows cosine fluctuations. The acceleration of the X, Y, Z directions reaches the maximum at 2.83s, 0.73s and 0.73s respectively, and reaches the minimum at 1.45s, 2.10s and 2.26s respectively.

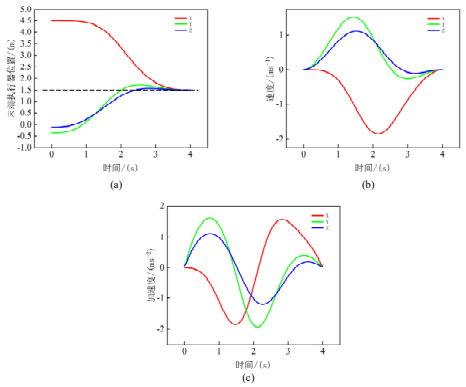

Figure 15. Quintic polynomial interpolation (a) End effector position (b) Velocity (c) Acceleration

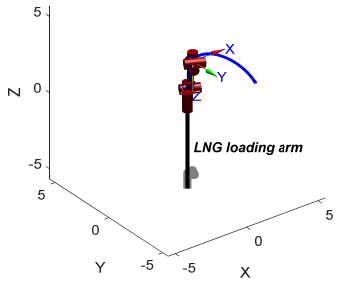

Figure 16. Quintic polynomial interpolation trajectory

ISSN: 2688-8645

Figure 16 shows the automatic docking trajectory of the LNG loading arm planned by quintic polynomial interpolation, which is a spatial arc. Compared with the spatial straight line, the spatial arc has a higher fault tolerance rate and is more in line with the requirements of engineering practice.

To further explore the quintic polynomial interpolation docking trajectory, the position, velocity and acceleration of the end effector in Figure 15 are decomposed into the motion states of each joint through forward kinematics solution, as shown in Figure 17,Figure 18and Figure 19.

Figure 17 is the position diagram of each joint during the quintic polynomial interpolation docking trajectory, which is overall smooth without abrupt changes. Among them, joint2, joint3, joint5 and joint6 have the same change trend, and joint1 and joint4 have the same change trend.

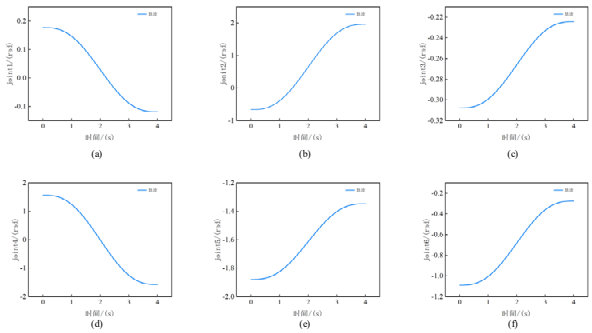

Figure 17. Joint positions

Figure 18 is the joint velocity during the quintic polynomial interpolation docking trajectory. joint1, joint2, joint3 and joint6 have the same change trend showing sinusoidal changes, and joint4 and joint5 have the same change trend showing cosine changes. The velocity of joint1~6 at the initial and final positions is 0 rad/s and all reach the extreme value at 1.98s and 2.02s. The velocity of joint4 is very small, almost in a static state.

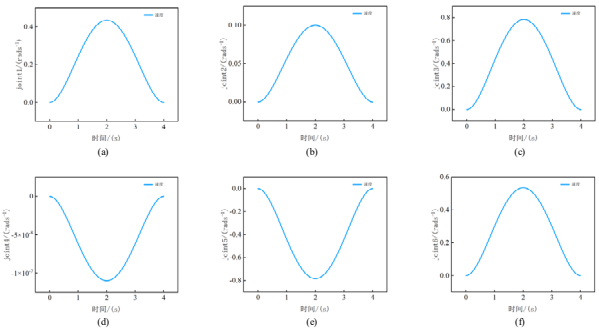

Figure 18. Joint velocities

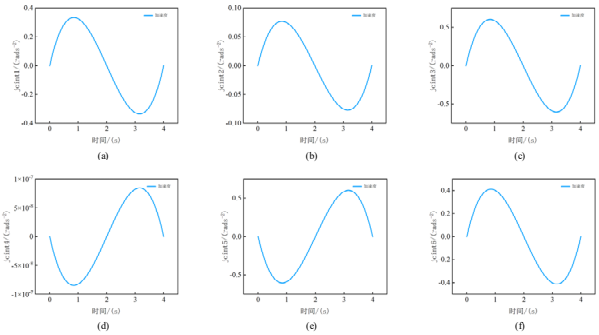

Figure 19. Joint accelerations

ISSN: 2688-8645

Figure 19 is the joint acceleration during the quintic polynomial interpolation docking trajectory. joint1, joint2, joint3 and joint6 have the same change trend showing sinusoidal changes, and joint4 and joint5 have the same change trend showing cosine changes. Similar to the velocity diagram, the acceleration of joint4 is also very small. joint1~3 and joint5~6 reach the acceleration extreme value at the same time, which is 0.89s and 3.19s respectively. During the entire docking process, the acceleration of each joint has no abrupt changes or fluctuations, which indicates that the quintic polynomial interpolation trajectory effectively controls the smoothness of joint motion and ensures the continuity and stability of the entire motion process. Compared with the cubic polynomial interpolation trajectory, the quintic polynomial interpolation trajectory realizes the posture control of the end effector, and the planned trajectory has higher fault tolerance. The position, velocity and acceleration perform more naturally, smoothly and stably during the docking process. To further analyze the stability of the quintic polynomial interpolation during the docking process, the acceleration is further differentiated with respect to time in a generalized way to obtain the impact diagram of the end effector in Figure 20. It can be seen from Figure 20 that the quintic polynomial interpolation trajectory has sharp points in the Y and Z directions at the initial moment and in the X, Y and Z directions at the final moment, but the sharp points only appear at an instantaneous moment, and the end effector of the LNG loading arm changes steadily at other moments.

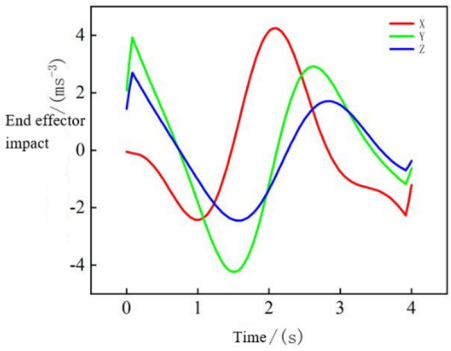

Figure 20. End effector impact

The results show that the quintic polynomial trajectory planning algorithm generates a continuously differentiable spatial trajectory curve in the Cartesian space, and its position, velocity and acceleration parameters all show C^4 continuity in the time domain. The algorithm not only meets the requirements of smooth transition of the end effector's pose, but also maintains the jerk index within the engineering allowable range during the entire docking process except for the limited magnitude of impact at the initial and final moments. Through a comprehensive evaluation, the quintic polynomial algorithm is superior to other comparison algorithms in terms of trajectory continuity, controller compatibility and dynamic characteristics. The generated time-domain parameter curve has no step mutation phenomenon, which conforms to the technical requirements for motion stability in HG/T21608-2012 Technical Requirements for Liquid Loading Arm Engineering[11],and provides a theoretical basis and feasible trajectory planning scheme for the design of high-precision motion controllers in the follow-up.

4. Summary

(1) In the modeling process, this paper adopts the modified D-H method to establish the kinematic model of the LNG loading arm and construct the corresponding D-H parameter table. By analyzing the joint structure and its motion range of the loading arm, the distribution law of its degrees of freedom and kinematic parameters is determined.

(2) According to the kinematic model and D-H parameter table of the LNG loading arm, this study uses the Matlab Robotics Toolbox to compare and analyze four typical trajectory planning algorithms (cubic spline interpolation, quintic spline interpolation, cubic polynomial and quintic polynomial). Compared with the cubic spline interpolation and cubic polynomial algorithms, the quintic polynomial trajectory planning algorithm generates a continuously differentiable spatial trajectory curve in the Cartesian space, and its position, velocity and acceleration parameters all show C^4 continuity in the time domain.

References

[1] Ye Dai, Chaofang Xiang, Yuan Zhang, et al. A Review of Spatial Robotic Arm Trajectory Planning[J]. Aerospace, 2022, Vol.9(7): 361.

[2] Yang Mei, Zeng Guiying, Ren Yong, et al. Accessibility and Trajectory Planning of Cutter Changing Robot Arm for Large-Diameter Slurry Shield[J]. MECHANIKA, 2023, Vol.29(3): 214-224.

[3] Zhao Yanling, Zhou Enwen, Zhang Jingwei, et al. Design and motion analysis of a small motor stator multi-wire paralleled winding hybrid robot[J]. Mechanical Sciences, 2021, Vol.12(2): 1005-1016.

[4] Li H, Zheng Z Z, Huang S Z, et al. Trajectory planning and simulation of industrial robot based on ROS[J]. Modular Machine Tool & Automatic Manufacturing Technique, 2018(12):59-62.

[5] Ren J, Wu Z H, Cao Q Y. Trajectory planning and simulation of ER50 robot based on MATLAB Robotics Toolbox[J]. Machinery Design & Manufacture, 2022(8): 33-36.

[6] Cai G Q, Hao R L, Zhou L J, et al. Workspace simulation and trajectory planning of food handling robot[J]. Food and Machinery, 2022, 38(9): 114-119.

[7] Gao Z R, Wang L, Lei J D, et al. Robot trajectory optimization based on polynomial interpolation algorithm[J]. Value Engineering, 2021, 40(26): 157-159.

[8] Sherif I Abdelmaksoud, Mohammed H Al-Mola, Ghulam E Mustafa Abro, et al. In-Depth Review of Advanced Control Strategies and Cutting-Edge Trends in Robot Manipulators: Analyzing the Latest Developments and Techniques[J]. IEEE Access, 2024, Vol.12: 47672-47701.

[9] Ma Boyu, Zhou Chunyu, Liu Yang, et al. A Comprehensive Derivation of Quintic Spline Interpolation and Its Applications to 3-D Collision-Free Trajectory Generation[A]. 2024 IEEE International Conference on Real-time Computing and Robotics (RCAR)[C], 2024.

[10] Pu Yasong, Shi Yaoyao, Lin Xiaojun, et al. Joint motion planning of industrial robot based on hybrid polynomial interpolation[J]. Xibei Gongye Daxue Xuebao, 2022, Vol.40(1): 84-94.

[11] HG/T 21608-2012. Technical Requirements for Liquid Loading Arm Engineering[S]. Hualu Engineering & Technology Co., Ltd, 2012.